Origin of nonlinear magnetoelectric response in rare-earth orthoferrite perovskite oxides

Alireza Sasani [1] Jorge Íñiguez,[2,3] and Eric Bousquet[1]

[1]*Physique Théorique des Matériaux, QMAT, CESAM, Université de Liège, B-4000 Sart-Tilman, Belgium*
[2]*Materials Research and Technology Department, Luxembourg Institute of Science and Technology (LIST),
5 avenue des Hauts-Fourneaux, L-4362, Esch/Alzette, Luxemburg*
[3]*Department of Physics and Materials Science, University of Luxembourg, Rue du Brill 41, L-4422 Belvaux, Luxembourg*

We report a theoretical study of the nonlinear magnetoelectric response of $GdFeO_3$ through an analytical approach combined with a Heisenberg model, which is fitted against first-principles calculations. Our theory reproduces the nonlinear change of polarization under applied magnetic field reported experimentally such that it allows us to analyze the origin of the large responses in different directions. We show that the nonlinear character of the response in these materials originates from the fact that the antiferromagnetic order of Gd atoms changes nonlinearly with respect to the applied magnetic field. Our model can be generalized to other materials in which the antiferromagnetic ordering breaks inversion symmetry.

I. INTRODUCTION

Magnetoelectric (ME) materials are compounds in which there is a coupling between magnetic field (magnetization) and electric field (polarization) [1,2]. Magnetoelectricity is a sough-after material's response because it allows controlling the magnetic properties using an external electric field or, the other way around, to control the polarization using an external magnetic field and, hence, it can have a plethora of possible applications in spintronics, sensors, etc. [3–5]. In particular, these materials can be used to improve memory devices by enhancing the speed of the device performance together with reducing its energy consumption [5,6].

Since the first experimental observation of the ME effect by Astrov [7] there have been many works to find the ME effects in other materials but it appeared that most of these ME responses were very small to be considered practical [4,5,8,9]. So far, the discovered ME materials have either a small coupling [10], or a very low-performance temperature [11], which hinders putting them into applications. Different paths are introduced to enhance the ME response of materials. To name a few, we have structural softness through epitaxial strain [12,13] or solid solutions [14] or making artificial structures and superlattices [15,16].

Bulk multiferroic (MF) materials are a subclass of MEs in which there exist two ferroic orders in the same phase, i.e., ferroelectricity along with ferromagnetic (FM) or antiferromagnetic (AFM) order [17]. This class of materials are divided into two groups, namely, type-I and type-II [18]. Type-II MFs are materials in which the magnetic ordering is the mechanism that breaks the inversion symmetry causing ferroelectricity. Hence, in type-II MFs a strong coupling between magnetism and polarization is present by construction (since the magnetization breaks inversion symmetry, the polarization is sensitive to a magnetic field), resulting in strong

ME responses with respect to type-I MFs where the coupling is more indirect. The reported ME responses for these materials show that indeed the strongest ME responses are found in type-II MFs [11,19–22]. In a type-II MF, the ME response can result from either noncollinear spin ordering, in which we expect small polarization since it arises from spin-orbit coupling (SOC) ($10^{-2} \mu C/cm^2$); or it can result from inversion symmetry breaking due to collinear ordering of the spins. In the latter case, the mechanism can be other than SOC, like exchange striction, which typically yields large polarization (one to two orders of magnitude larger) compared to the first mechanism. Some of the rare-earth orthoferrites (e.g., $GdFeO_3$) are of type-II multiferroics, in which the collinear ordering of spins creates the polarization. Hence, they have larger polarization compared to other type-II MFs as well as larger ME responses [23]. Although the temperature at which the multiferroicity appears in rare-earth orthoferrites is very low (it requires that the rare-earth spins become ordered), their ME responses are sizable [21,22]. These rare-earth orthoferrite materials have such a strong coupling that makes it possible to control ferroelectric order using magnetic fields or to control the magnetic ordering using electric fields [21]. However, the exact origin of their large responses have not been fully understood from first-principles or model Hamiltonian. The lack of such calculations is due to the complexity associated with the presence of two different and coupled magnetic sublattices. Besides, the rare-earth magnetism comes from f electrons, which are difficult to handle within density functional theory (DFT) calculations [24,25].

In this paper we report a simulation study of the microscopic origin of the large nonlinear ME response of $GdFeO_3$. Experimentally it has been observed that the polarization goes from 0.12 $\mu C/cm^2$ to 0 $\mu C/cm^2$ under an applied magnetic field of 3.7 T [21]. If we extrapolate an effective linear response in the unit of ps/m by calculating $\frac{\Delta P}{\Delta B}$ between 0

and 3.7 T, we obtain an effective amplitude of about 406 ps/m, i.e., the same order of magnitude as in the linear ME crystal TbPO$_4$ (730 ps/m, which is among the largest linear ME responses observed in single crystal) [26]. Although this response is not the strongest nonlinear ME response reported in materials [27,28], understanding its microscopic mechanism will help in designing and engineering other large ME materials. To tackle this problem from a simulation viewpoint, we first derive an analytical form of the ME response of this material using a Heisenberg Hamiltonian and fit the parameters by DFT calculations. Then, we report the results obtained through classical spin dynamics to calculate the ME response and the polarization of these materials under an applied magnetic field. Our results reproduce the response observed experimentally on GdFeO$_3$, i.e., the fully nonlinear response and the appearance of two regimes, associated with a magnetic phase transition under the applied magnetic field.

II. TECHNICAL DETAILS

In this paper, we have used a Heisenberg model that has been derived previously by us in Ref. [29], which includes both rare-earth and transition metal site interactions [superexchange and Dzyaloshinskii-Moriya interactions (DMI)]. This model is fitted against DFT calculations [30,31] of the $Pna2_1$ phase of GdFeO$_3$. We used the Vienna Ab Initio Simulation Package (VASP) [32,33] and its projected augmented wave implementation [34]. We used the so-called generalized gradient approximation (GGA) of the PBEsol flavor [35] for the exchange-correlation functional and added a Hubbard U correction [36] on Fe and Gd of respectively 4 eV and 5 eV as well as a J parameter of 1 eV on Fe. Since the behavior that we are interested in is arising from exchange interactions, we have chosen Hubbard interaction parameters (U) so that we get the closest Néel temperature compared to experiments. All the calculations were done considering noncollinear magnetism and including the spin-orbit interaction. The calculations were converged with a 6×6×4 mesh of k points for sampling the reciprocal space and cut-off energy on the plane wave expansion of 700 eV (giving a precision of less than 5 μeV on the single-ion anisotropy and the DMIs).

The calculations of the superexchange interactions were done using Green's function method as implemented in the TB2J code [37]. In this method the maximally localized Wannier function [38] as implemented in WANNIER90 [39] are calculated using DFT (VASP interface to Maximally localized Wannier functions) and, using these Wannier functions and the Green's function method, the superexchange parameters are calculated. Some of these superexchange interactions were compared to the ones calculated using total energy to ensure the consistency of the method. To determine the DMI amplitudes, we have calculated the energy of different spin configurations as described by Xiang *et al.* [40]. All of the fitted magnetic interaction parameters were used to do spin dynamics with the VAMPIRE code [41]. In this code the Landau-Lifshitz-Gilbert (LLG) equation for the spin dynamics

$$\frac{\partial S_i}{\partial t} = \frac{\gamma}{1+\lambda^2} \left[S_i \times B_{\text{eff}}^i + \lambda S_i \times \left(S_i \times B_{\text{eff}}^i \right) \right] \quad (1)$$

is solved numerically. The ground state (lowest energy solution at T = 0 K) for each of the calculations (with applied magnetic field) is found by minimizing the energy with respect to the magnetic order.

The calculation of the polarization is done using the Berry phase approach as implemented in VASP [42,43]. In GdFeO$_3$, the main magnetic ground state of Fe sublattice is a G-type AFM ordering with a modulation vector of [0.5,0.5,0.5] (with respect to the 5 atoms cubic perovskite unit cell). On the top of this main G-type AFM order there are also canting due to the DMI (giving either a weak FM canting, or F-type, a weak A-type AFM canting with [0.5,0,0] modulation vector or a weak C-type AFM canting with [0.5,0.5,0] modulation vector). The Gd atoms also order in G-type at temperatures lower than 2.5 K.

To find the change of polarization as a function of the G-type order, we rotated the magnetic ordering of the Gd sublattice from G-type in the x direction (i.e., G$_x$) to the F-type in the z direction (i.e., F$_z$). The process of the rotation is done by constraining the magnetic order [44] on the Gd sublattice and relaxing atomic structure and Fe sublattice magnetic moments. At each step, we have used the berry phase to calculate the polarization of the magnetic structure.

Before analyzing the results obtained with the fitted model, we start with an analytical discussion of the magnetic interactions present in GdFeO$_3$.

III. THEORETICAL DERIVATION

In this section, we derive an analytical expression of the ME response of the GdFeO$_3$. This ME response is originating from the exchange striction. To derive the ME response, we use the fact that the interaction between the G-type (or A-type) magnetic order of the Gd sublattice and the G-type (or A-type) order of the Fe sublattice is the driving force that breaks the inversion symmetry, which causes the polarization in rare-earth orthoferrites [21,23,45]. Hence, we will consider the polarization to be a function of the G-type order of the Gd site such that we can expand the polarization in terms of the corresponding order parameter (Fe G-type is considered to be constant in this process). From this assumption, we can write the ME response in these structures using the following relations:

$$\frac{\partial P_i}{\partial B_l^{\text{app}}} = \frac{\partial P_i}{\partial G_j^R} \frac{\partial G_j^R}{\partial B_l^{\text{app}}}, \quad (2)$$

where B_l^{app} is the applied magnetic field in the l direction, P_i is the polarization in the i direction and G_j^R is the magnitude of the G-type order on rare-earth site in the j direction.

To probe the variation of G-type order with respect to the magnetic field, $\frac{\partial G_j^R}{\partial B_l^{\text{app}}}$, we use the general Heisenberg model developed by us for RMO_3 crystals (R = Rare-earth, M = Fe or Cr) [29] but using the data fitted from DFT calculations done on GdFeO$_3$.

In deriving the ME response, we have neglected the changes of the Fe sublattice. The magnetic field should move the Fe sublattice from the AFM order to the FM order but this competes with the strong superexchange interactions between Fe atoms that maintain the G-type AFM order. The Fe sublattice has a Néel temperature larger than 600 K, which

corresponds to an effective magnetic field of the order of 10^2 T (due to the superexchange). Hence, this effective magnetic field is much larger than the fields relevant in this work (up to 5 T) and we can neglect the Fe sublattice changes in our theoretical model with a good approximation. additionally, our spin dynamics simulations confirm that the magnetic order of the Fe sublattice is almost not affected by the range of magnetic fields that we are interested in (see Fig. 3).

The energy of rare-earth spins per formula unit can be derived from the Heisenberg Hamiltonian to obtain:

$$H_{\text{Heis}}^R = -3J^R \left(G_i^R\right)^2 + 3J^R\left(F_j^R\right)^2 \\ - K^R\left(G_i^R\right)^2 - B_l^{\text{app}} F_j^R \delta_{jl} - B_m^{RM} F_j^R \delta_{mj}, \quad (3)$$

where J^R is the exchange interaction between rare-earth sites and G_i^R and F_j^R are the G-type AFM and weak FM orders on rare-earth in the i and j directions respectively, K is the single ion anisotropy in the i direction. The interaction of Gd and Fe spins can be reduced to an effective magnetic field B_m^{RM}, which can be written as follows [29,46]:

$$B_m^{RM} = 8J^{RM} F_m^M + 8\left(d_y^{RM} G_{m'}^M\right), \quad (4)$$

This formula represents the effective field in m direction on Gd sublattice from Fe. J^{RM} is the exchange interaction between Gd and Fe and the d_y^{RM} is the y component of DMI between rare-earth and transition metal cations (DMI has the largest component in y direction [29]). $G_{m'}^M$ represents G-type order in direction m' that is perpendicular to m and y. We consider the effective magnetic field B_m^{RM} to be in the same direction as the applied magnetic field, or small compared to it such that it can be neglected. In the case where the applied field is in the z direction and the rare-earth orders in G_x order, the B_m^{RM} and the applied magnetic field are in the same direction [29,46]. When the applied field is in the x direction, B_m^{RM} and the applied field are perpendicular to each other before the phase transition (in which we can consider B_m^{RM} to be negligible compared to the applied magnetic field), while after the phase transition they will be in the same direction.

We can minimize the energy with the following constraint using Lagrange multipliers (the constraint is coming from considering the magnitude of the spin as normalized with the spin magnetic moments of each atom, i.e., $5\mu_B$ for Fe and $7\mu_B$ for Gd):

$$\left(G_i^R\right)^2 + \left(F_j^R\right)^2 = 1, \quad (5)$$

which gives us the G_i and F_j orders as a function of the applied magnetic field:

$$G_i^R = \pm\sqrt{1 - \left(\frac{B_l^{\text{eff}}}{J_P}\right)^2} \quad (6)$$

$$F_l^R = \frac{B_l^{\text{eff}}}{J_P}. \quad (7)$$

where $B_l^{\text{eff}} = B_l^{\text{app}} + B_l^{RM}$ (since $B_l^{RM} = $ constant, $\frac{\partial G_j^R}{\partial B_l^{\text{eff}}} = \frac{\partial G_j^R}{\partial B_l^{\text{app}}}$) and $J_P = 12J^R + 2K^R$ in our equations. From these expres-

sions we can obtain the following term:

$$\frac{\partial G_j^R}{\partial B_l^{\text{eff}}} = \mp \frac{\frac{B_l^{\text{eff}}}{J_P}}{\sqrt{1 - \left(\frac{B_l^{\text{eff}}}{J_P}\right)^2}}. \quad (8)$$

Now, we are left with the determination of the variation of P with respect to G_j^R: $\frac{\partial P_l}{\partial G_j^R}$. Because the exchange striction between the rare-earth site and the transition metal site is the interaction responsible for polarizing the material [21,23], we are going to use the energy expression for this interaction to derive the $\frac{\partial P_l}{\partial G_j^R}$. To derive this expression we use an energy expression written as a function of the change in the exchange interaction due to atomic displacement and elastic potential that resist against this deformation:

$$E_{\text{int}} = -4G_i^R G_j^M \epsilon_l^{ij} \Delta r_l^{ij} + \frac{1}{2}k\left(\Delta r_l^{ij}\right)^2 \quad (9)$$

where the change in exchange interaction (J_{ij}^{RM}) between R and M atoms is written as $\epsilon_l^{ij} \Delta r_l^{ij}$ (changes of J_{ij}^{RM} expanded to linear order). In this relation ϵ_l^{ij} is the constant of proportionality and Δr_l^{ij} is the magnitude of the change of l component of the position vector between the atoms. k in this equation represents the elastic constant. By minimizing Eq. (9) we can write the equilibrium displacement as follows:

$$\Delta r_l^{ij} = \epsilon_l^{ij} \frac{4G_i^R G_j^M}{k}. \quad (10)$$

If we expand the l component of the polarization and keep the linear order with respect to the atomic displacements away from the center of symmetry, we can write it as follows:

$$P_l = \zeta_l^{ij} \Delta r_l^{ij} \quad (11)$$

From Eq. (11) and Eq. (10) we can write the polarization in l direction as

$$P_l = 4\delta_l^{ij} G_i^R G_j^M \quad (12)$$

Where we have used the $\delta_l^{ij} = \frac{\zeta_l^{ij} \epsilon_l^{ij}}{k}$. If we consider the isotropic exchange interactions in this equation (i.e., i = j), we can derive the following relation:

$$\frac{\partial P_l}{\partial G_j^R} = 4\delta_l^{jj} G_j^M. \quad (13)$$

To determine the strength of the change of polarization as a function of the magnitude of the G_x ordering of rare-earth [as Eq. (13)], we performed DFT calculations. We have calculated the polarization for different magnetic ordering of Gd atoms by changing their spin order from G_x to F_z by rotating it slowly. In Fig. 1 we report the results, i.e., the change of polarization as a function of the G_x order magnitude of Gd atoms as we go from G_x to the F_z order. We can notice the linear relation between G-type order magnitude and the polarization, which proves that the Eq. (12) is a good estimation of the polarization of the materials as a function of G-type order magnitude.

By fitting the Eq. (13) with the results of Fig. 1, we can extract the coefficients of this equation. From this, we obtain $\frac{\partial P_z}{\partial G_x^R} = 0.328 \ \mu\text{C cm}^{-2}\mu_B^{-1}$ with the polarization in the z direction, which is perpendicular to G_x magnetic ordering (from now on we will consider the polarization in the z direction).
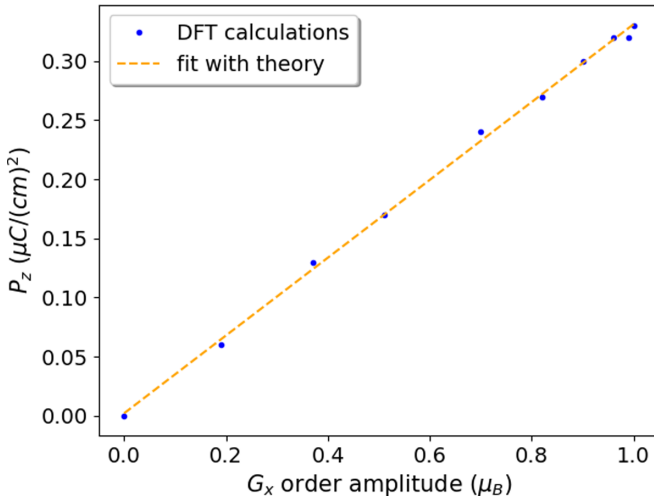
FIG. 1. Polarization of the GdFeO$_3$ as a function of magnitude of G_x order in the material. We also have shown the fitted line with the theory using dashed-orange line.

$$F_xC_yG_z\ (\Gamma_2) \qquad G_xA_yF_z\ (\Gamma_4)$$

FIG. 2. Schematic presentation of the two main magnetic phases of GdFeO$_3$: (a) Γ_2 and (b) Γ_4. These orders are for Fe sublattice while Gd sublattice ordering are presented by G_xA_y and G_z where inversion symmetry is broken. In this figure the G-type is the main component of the spin and the others letters represent the canted orders due to the DMI, the subscript gives the direction in which each order develops [47].

With this coupling term at hand, we can explore how the crystal responds to an applied magnetic field with the Heisenberg model and deduce how the polarization changes, i.e., the ME response. We use the same applied field conditions as reported experimentally for GdFeO$_3$ by Tokunaga *et al.* [21].

We can now have following analytical expression for the ME response:

$$\frac{\partial P_z}{\partial B_l^{\text{eff}}} = \mp \frac{4\delta_z^{jj} G_j^M \frac{B_l^{\text{eff}}}{(J_P)^2}}{\sqrt{1 - \left(\frac{B_l^{\text{eff}}}{J_P}\right)^2}} \qquad (14)$$

where the negative and positive signs are for the positive and negative direction of the applied magnetic field respectively. In this equation, we consider $B_l^{\text{eff}} < J_p$, which means the Gd atoms are not completely FM ordered. This assumption is a valid assumption, since we are studying the response of the system in this regime.

Our derivation allows us to understand the origin of the nonlinear behavior. Since the calculated ME response is from two terms, (i.e., $\frac{\partial P_i}{\partial G_j^R}$ and $\frac{\partial G_j^R}{\partial B_l^{\text{app}}}$) we can see that the ME response is nonlinear because the AFM order changes nonlinearly under an applied magnetic field (i.e., $\frac{\partial G_j^R}{\partial B_l^{\text{app}}}$ term) and we can expect this nonlinear behavior for all the cases where the AFM order breaks the inversion symmetry (this should be the case for the A-type AFM order and the E-type AFM order). While the AFM order creates a nonlinear ME response, the FM order that drives ferroelectricity will have a linear ME response before magnetization saturation [since the FM order changes linearly with respect to an applied magnetic field, see Eq. (7)]. Another point to mention is the fact that the A-type AFM ordering of the rare-earth site can also break the inversion center in these structures and can induce nonlinear polarization. If we consider the ME response from this ordering we should change the the value of J_p (i.e., $12J^R + 2K^R$) by $4J^R + 2K^R$ in the ME response.

By integrating Eq. (14) with respect to the magnetic field, we can calculate the polarization as a function of the magnetic

field for these materials using the initial values obtained from DFT. This integration gives the following final analytical expression:

$$P_z(B_l^{\text{eff}}) = 4\delta_z^{jj} G_j^M \left(\sqrt{1 - \left(\frac{B_l^{\text{eff}}}{J_P}\right)^2}\right)$$

$$= 4\delta_z^{jj} G_j^M G_j^R \qquad (15)$$

In the second equation, we are using Eq. (6). Now that we have analyzed analytically the ME response of rare-earth perovskites in the magnetic phases as present in ferrites and chromites, in the next section we present our numerical results coming from the simulations for GdFeO$_3$.

IV. SIMULATIONS

In this section, we present the results of the spin dynamics simulations to study numerically the effect of the applied magnetic field on magnetism and the resulting ME response. For GdFeO$_3$, the magnetic ground state is as shown in Fig. 2(b) in which the main spin component is G_x [i.e., $(G_xA_yF_z)$ for Fe and (G_xA_y) for Gd] and it has a small FM canting in the z direction (i.e., F_z). When the magnetic field is applied in the z direction, the magnetic ordering of the Gd sublattice changes slowly from G$_x$ to F$_z$. When the applied magnetic field is in the x direction, it induces an FM order in the x direction, which is not allowed by symmetry in the $(G_xA_yF_z)$ state. Hence, by increasing the magnitude of the applied magnetic field in the x direction, the magnitude of energy coming from the $F_xB_x^{\text{app}}$ interaction increases, and once this energy is large enough to compensate the energy difference between the two magnetic states (i.e., G_z and G_x) a phase transition takes place for the Gd sublattice by rotating it from G_x to G_z. During this phase transition, the magnetic order of the Fe sublattice stays in its $G_xA_yF_z$ phase while the Gd sublattice changes to F_xG_z). This spin-flip phase transition can be seen as a change in magnetic anisotropy for Gd sublattice from x to z direction. We present the results for two different regimes (i.e., B_z^{app} and B_x^{app}) in the two following sections.
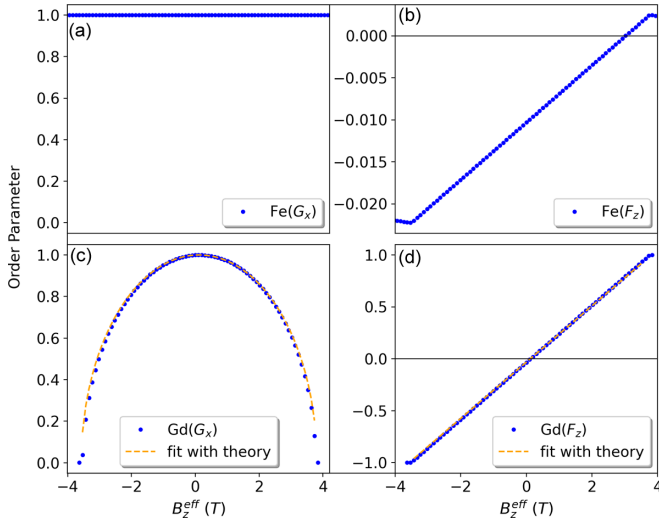
FIG. 3. Fe and Gd site magnetic ordering for spins in x and z direction as a function of applied magnetic field in z direction. The left panel shows the x component of the spins and the right one shows the z component of the spins.

A. Magnetic fields perpendicular to the G_x direction

In this part we discuss the ME response of GdFeO$_3$ for a magnetic field applied perpendicular to the direction of the Gd spins with G_x order (i.e., magnetic field in z direction).

In Figs. 3(a) and 3(b) we show the spin dynamics results of the effect of an external magnetic field on Fe sublattice. We notice that the Fe sublattice does not change much as the magnetic field is applied to the structure, we can only observe a small change in its weak FM canting. This result shows that we can neglect the Fe magnetic order changes effects on the ME response since the effects for Gd sublattice are much larger.

In Figs. 3(c) and 3(d) we report the effect of the applied magnetic field in the z direction on the Gd sublattice. We can see a continuous decrease of the G_x ordering and an increase of the F_z. Hence, the applied magnetic field can fully magnetize the Gd parallel to the field direction. Beyond a critical field of 4 T, we can see that the ground state G_x order has disappeared, the magnetic field having fully magnetized all the Gd moments in the same direction. This transition is fully consistent with the experimental results of Ref. [21].

To check the consistency of the spin dynamics results with the analytical solution that we have obtained in the previous section, we fitted the results of the FM order (z component of the Gd spin) with Eq. (7) to obtain the J^R, K^R, and B_l^{RM} parameters. The orange-dashed line in Fig. 3(d) shows the resulting fit that is in good agreement with the spin dynamics results (blue dots). We then used these parameters and put them in Eq. (6) and plotted the results in Fig. 3(c) for the G_x Gd spin. The values for the parameters obtain from the fit with spin dynamics are close to the values calculated from DFT. As we can see these results agree well with the spin dynamics simulations.

Having calculated the required coefficients for the magnetic response, we can calculate the ME response from Eq. (14). In Fig. 4 we report the evolution of the change of
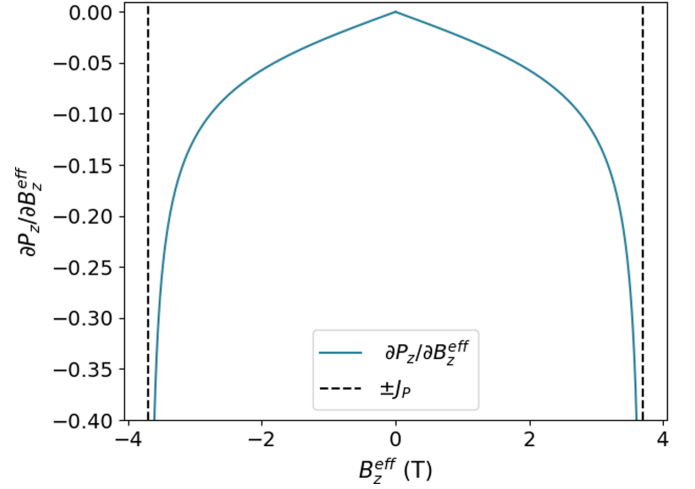
FIG. 4. Nonlinear ME response of GdFeO$_3$ orthofrrites plotted according to Eq. (14) where we can see a divergence in the response as applied magnetic field strength get closer to J_p.

polarization versus the applied magnetic field. We can see that the change of polarization response is negative (i.e., the magnetic field reduces the polarization), symmetric for each magnetic field direction, and diverges when approaching the critical field where the Gd order goes from G_x to F_z. This critical field is directly related to the amplitude of the Gd exchange interaction (J^R), which governs the energy change associated with the change of the Gd magnetic order. This corresponds to the phase transition from the polar $m'm2'$ ($Pna2_1$) phase to the para-electric $m'm'm$ ($Pnma$) phase.

In Fig. 5 we show the polarization versus the magnetic field of GdFeO$_3$ as obtained from Eq. (15). We obtain that the polarization decreases nonlinearly for both directions of the field and reaches zero at the critical magnetic field where the crystal goes to the $Pnma$ para-electric phase. In this figure, we have also included the magnetization of the crystal
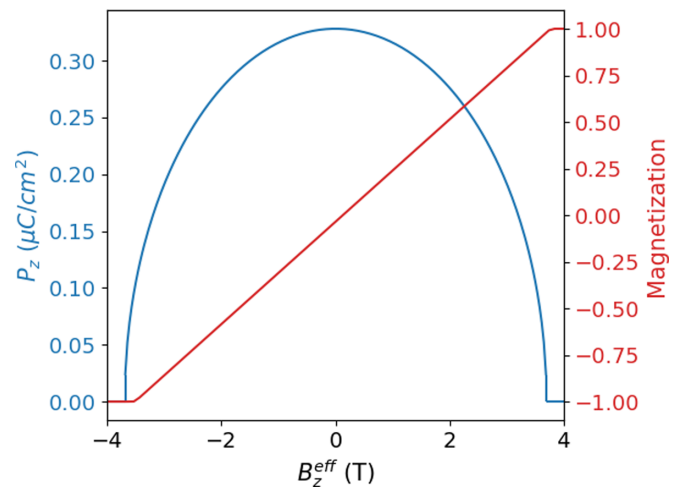
FIG. 5. In the figure, the blue curve represents the change of polarization of GdFeO$_3$ as a function of the effective magnetic field. The red line shows the magnetization of the GdFeO$_3$ coming from F_z ordering of Gd sublattice.
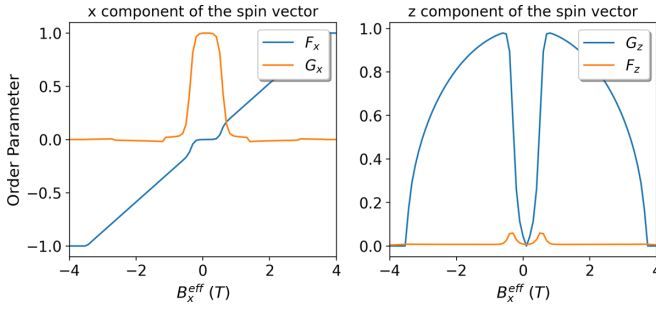
FIG. 6. The Gd site magnetic ordering as a function of applied magnetic field in x direction. For the magnetic field of more than 0.7 T, we can see the sudden drop of G_x (the orange line in x component of spin), which is accompanied by an increase in G_z (blue line in z component of spin).

FIG. 7. Change of polarization as a function of applied magnetic field in x direction where we can see the ordering of Gd site in G_x before phase transition and in G_z with lower polarization after phase transition.

coming from the Gd where we can see that when the Gd sublattice is ferromagnetically ordered, the polarization vanishes. This result is in very good agreement with the experimental results of Tokunaga *et al.* [21], which also proves that our model describes correctly the ME response of this material.

B. Magnetic field parallel to the G_x direction

In this section we discuss the ME response of GdFeO$_3$ for an applied magnetic field parallel to the direction of the Gd G_x magnetic order. Similar to the applied field along the z direction, our simulations give that the magnetic ordering of the Fe site is not strongly affected by the applied magnetic field along the x direction such that we can neglect its changes. In Fig. 6 we report the evolution of the Gd sublattice spin when we apply a magnetic field in x direction. We can see that for a critical magnetic field of about 0.7 T, the Gd goes thorough a spin-flip phase transition from G_x (orange line) to G_z (blue line). In this structure, the Gd atoms prefer to be in G_x state due to single-ion anisotropy and also the effective field of Fe. By applying a magnetic field in the x direction we lower the energy of the G_z state by $B_x F_x$ (where F_x is a weak canted moment characteristic of the G_z state) and once this energy is larger than the energy difference between G_x and G_z, we will have a phase transition. Beyond this phase transition, the Gd spins start to be more and more FM and it becomes fully magnetized for the amplitude of the 4 T magnetic field.

As done previously for the applied field along the z direction, we can also calculate how the polarization is affected by the applied field along the x direction and so the ME response. In Fig. 7 we report the evolution of the polarization versus the applied magnetic field along x. We encounter a nonlinear ME response again where the polarization is decreased for both directions of the field. We, however, observe two regimes, one between 0 and $\pm$0.7T where the polarization is approximately constant and not affected by the field. Exactly at $\pm$0.7 T we observe a sharp polarization drop from 0.36 $\mu C/cm^2$ to 0.05 $\mu C/cm^2$, a reduction by a factor of 5 (calculated from DFT) due to the transition of Gd sublattice from the G_x to the G_z phase.

Then, beyond $\pm$0.7 T we have a nonlinear further reduction of the polarization down to zero when the Gd is fully magnetized by the field along the x direction. The polarization will
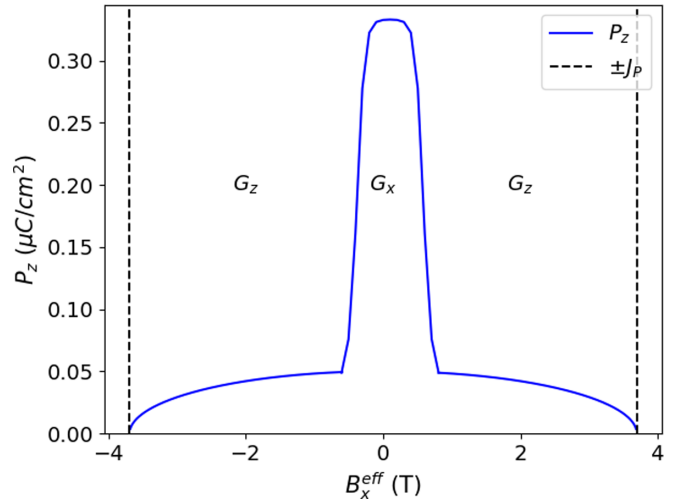
change like Eq. (15) for the range of fields between 0.7 T and 4 T with a different exchange coupling: in the first case (for B_z) we had both Gd and Fe atoms main spin component in the x direction and we were considering $\delta_z^{xx} = \frac{\zeta_z^{xx} \epsilon_z^{xx}}{k}$; instead, now we will have $\delta_z^{zx} = \frac{\zeta_z^{zx} \epsilon_z^{zx}}{k}$ (Fe in G_x and Gd in G_z), which is much smaller than the first δ_z^{xx} hence resulting in a smaller polarization for this part. The ME response will also be similar to Eq. (14) for magnetic fields higher than 0.7 T.

It has been experimentally claimed [21] that the Fe sublattice rotates for an applied field in the x direction. Our DFT calculations shows that if we rotate the Fe sublattice in the same direction as the Gd sublattice, we will not have a sudden drop of the polarization (because the polarization is directly proportional to the exchange interaction and here $J_{zz} \approx J_{xx}$). The fact that the polarization drops in the experiment would then come from the rotation the Gd sublattice alone. Hence, based on our DFT calculations, we conclude that the Fe sublattice does not rotate in this regime. Our results (with the Fe sublattice not rotated) reproduce well the experiments of Tokunaga *et al.* [21] where two regimes of nonlinear ME response were also observed with a polarization drop around the critical field of 0.7 T and a disappearance of the polarization beyond a critical field of about 4 T.

V. CONCLUSION

In this paper, we have analyzed the magnetoelectric response of the rare-earth orthoferrite perovskite oxides through theoretical methods based on DFT calculations, Heisenberg, and analytical models taking into account the exchange striction that induces the polarization. With this analysis, we have shown that the nonlinear character of the magnetoelectric response of GdFeO$_3$ is coming from the fact that the G-type ordering that breaks the inversion center changes nonlinearly with respect to an externally applied magnetic field. When the applied magnetic field is along the z direction, the polarization reduces down to zero at a field of 4 T, i.e., when the Gd spins

are all aligned with the magnetic field in an FM state where the exchange striction is absent. When the applied magnetic field is along the x direction, the field is parallel to the main Gd G-type spin direction such that we observe two regimes: (i) from 0 to 0.7 T, the polarization is affected negligibly by the field, and (ii) at 0.7 T the Gd spin directions change from x to z direction (but keeping its G-type AFM ordering), which induces a strong reduction of the polarization. From 0.7 T to 4 T the polarization is reduced nonlinearly down to 0 when the Gd becomes ferromagneticaly aligned with the field along x. These two regimes and the nonlinear evolution of the polarization observed for the two directions of the applied magnetic field in GdFeO$_3$ is in good agreement with the experiments such that we are confident about the validity of the developed model.

Our analysis can be generalized to other rare-earth perovskites in which the polarization arises from the AFM ordering and the exchange striction effect. Our conclusions are also general for all materials where the AFM order breaks the inversion symmetry in the presence of two different magnetic sublattices. For example, Wang *et al.* [28] have reported the ME response of Fe$_2$Mo$_3$O$_8$ where the AFM order breaks the inversion symmetry through the exchange striction effect. The ME behavior is similar to what we have for GdFeO$_3$, i.e., giant and nonlinear with similar shapes of the polarization versus magnetic field curves. Additionally, for the systems in which the FM order breaks the inversion symmetry, the same analysis can be done but instead of having a nonlinear response, we will have a linear response that will be observed.

[1] L. D. Landau, E. M. Lifshitz, and L. P. Pitaevskii, *Electrodynamics of Continuous Media Volume 8*, Course of Theoretical Physics (Elsevier Science, Amsterdam, 1995).

[2] P. Curie, Sur la symétrie dans les phénomènes physiques, symétrie d'un champ électrique et d'un champ magnétique, J. Phys. Theor. Appl. **3**, 393 (1894).

[3] W. F. Brown, R. M. Hornreich, and S. Shtrikman, Upper bound on the magnetoelectric susceptibility, Phys. Rev. **168**, 574 (1968).

[4] S. Dong, J. M. Liu, S. W. Cheong, and Z. Ren, Multiferroic materials and magnetoelectric physics: Symmetry, entanglement, excitation, and topology, Adv. Phys. **64**, 519 (2015).

[5] N. A. Spaldin and R. Ramesh, Advances in magnetoelectric multiferroics, Nat. Mater. **18**, 203 (2019).

[6] N. A. Spaldin, Multiferroics beyond electric-field control of magnetism, Proc. R. Soc. A **476**, 20190542 (2020).

[7] D. N. Astrov, Discovery of the dectrically induced magnetoelectric effect, Theoret. Phys. (USSR) **38**, 984 (1960).

[8] M. Fiebig, Revival of the magnetoelectric effect, J. Phys. D **38**, R123 (2005).

[9] K. F. Wang, J. M. Liu, and Z. F. Ren, Multiferroicity: The coupling between magnetic and polarization orders, Adv. Phys. **58**, 321 (2009).

[10] J. Wang, J. B. Neaton, H. Zheng, V. Nagarajan, S. B. Ogale, B. Liu, D. Viehland, V. Vaithyanathan, D. G. Schlom, U. V. Waghmare *et al.*, Epitaxial BiFeO$_3$ multiferroic thin film heterostructures, Science **299**, 1719 (2003).

[11] T. Kimura, T. Goto, H. Shintani, K. Ishizaka, T. Arima, and Y. Tokura, Magnetic control of ferroelectric polarization, Nature (London) **426**, 55 (2003).

[12] J. C. Wojdeł and J. Íñiguez, Ab Initio Indications for Giant Magnetoelectric Effects Driven by Structural Softness, Phys. Rev. Lett. **105**, 037208 (2010).

[13] E. Bousquet and N. Spaldin, Induced Magnetoelectric Response in *Pnma* Perovskites, Phys. Rev. Lett. **107**, 197603 (2011).

[14] T. Bayaraa, Y. Yang, M. Ye, and L. Bellaiche, Giant linear magnetoelectric effect at the morphotropic phase boundary of epitaxial Sr$_{0.5}$Ba$_{0.5}$MnO$_3$ films, Phys. Rev. B **103**, L060103 (2021).

[15] H. J. Zhao, W. Ren, Y. Yang, J. Íñiguez, X. M. Chen, and L. Bellaiche, Near room-temperature multiferroic materials with tunable ferromagnetic and electrical properties, Nat. Commun. **5**, 4021 (2014).

[16] R. O. Cherifi, V. Ivanovskaya, L. C. Phillips, A. Zobelli, I. C. Infante, E. Jacquet, V. Garcia, S. Fusil, P. R. Briddon, N. Guiblin *et al.*, Electric-field control of magnetic order above room temperature, Nat. Mater. **13**, 345 (2014).

[17] H. Schmid, Multi-ferroic magnetoelectrics, Ferroelectrics **162**, 317 (1994).

[18] D. Khomskii, Classifying multiferroics: Mechanisms and effects, Physics **2**, 20 (2009).

[19] L. C. Chapon, G. R. Blake, M. J. Gutmann, S. Park, N. Hur, P. O. Radaelli, and S. W. Cheong, Structural Anomalies and Multiferroic Behavior in Magnetically Frustrated TbMn$_2$O$_5$, Phys. Rev. Lett. **93**, 177402 (2004).

[20] M. Kenzelmann, A. B. Harris, S. Jonas, C. Broholm, J. Schefer, S. B. Kim, C. L. Zhang, S. W. Cheong, O. P. Vajk, and J. W. Lynn, Magnetic Inversion Symmetry Breaking and Ferroelectricity in TbMnO$_3$, Phys. Rev. Lett. **95**, 087206 (2005).

[21] Y. Tokunaga, N. Furukawa, H. Sakai, Y. Taguchi, T.-H. Arima, and Y. Tokura, Composite domain walls in a multiferroic perovskite ferrite, Nat. Mater. **8**, 558 (2009).

[22] Y. Tokunaga, S. Iguchi, T. Arima, and Y. Tokura, Magnetic-Field-Induced Ferroelectric State in DyFeO$_3$, Phys. Rev. Lett. **101**, 097205 (2008).

[23] H. J. Zhao, L. Bellaiche, X. M. Chen, and J. Íñiguez, Improper electric polarization in simple perovskite oxides with two magnetic sublattices, Nat. Commun. **8**, 14025 (2017).

[24] A. Stroppa, M. Marsman, G. Kresse, and S. Picozzi, The multiferroic phase of DyFeO$_3$: An ab-initio study, New J. Phys. **12**, 093026 (2010).

[25] L. Chen, T. Li, S. Cao, S. Yuan, F. Hong, and J. Zhang, The role of 4f-electron on spin reorientation transition of NdFeO$_3$: A first principle study, J. Appl. Phys. **111**, 103905 (2012).

[26] Rivera, J.-P., A short review of the magnetoelectric effect and related experimental techniques on single phase (multi-) ferroics, Eur. Phys. J. B **71**, 299 (2009).

[27] S. H. Chun, Y. S. Chai, Y. S. Oh, D. Jaiswal-Nagar, S. Y. Haam, I. Kim, B. Lee, D. H. Nam, K.-T. Ko, J.-H. Park, J.-H. Chung, and K. H. Kim, Realization of Giant Magnetoelectricity in Helimagnets, Phys. Rev. Lett. **104**, 037204 (2010).

[28] Y. Wang, G. L. Pascut, B. Gao, T. A. Tyson, K. Haule, V. Kiryukhin, and S. W. Cheong, Unveiling hidden ferrimagnetism and giant magnetoelectricity in polar magnet Fe$_2$Mo$_3$O$_8$, Sci. Rep. **5**, 12268 (2015).

[29] A. Sasani, J. Iñiguez, and E. Bousquet, Magnetic phase diagram of rare-earth orthorhombic perovskite oxides, Phys. Rev. B **104**, 064431 (2021).

[30] P. Hohenberg and W. Kohn, Inhomogeneous electron gas, Phys. Rev. **136**, B864 (1964).

[31] W. Kohn and L. J. Sham, Self-consistent equations including exchange and correlation effects, Phys. Rev. **140**, A1133 (1965).

[32] G. Kresse and J. Furthmüller, Efficiency of ab-initio total energy calculations for metals and semiconductors using a plane-wave basis set, Comput. Mater. Sci. **6**, 15 (1996).

[33] G. Kresse and J. Furthmüller, Efficient iterative schemes for *ab initio* total-energy calculations using a plane-wave basis set, Phys. Rev. B **54**, 11169 (1996).

[34] P. E. Blochl, Projector augmented-wave method, Phys. Rev. B **50**, 17953 (1994).

[35] J. P. Perdew, A. Ruzsinszky, G. I. Csonka, O. A. Vydrov, G. E. Scuseria, L. A. Constantin, X. Zhou, and K. Burke, Restoring the Density-Gradient Expansion for Exchange in Solids and Surfaces, Phys. Rev. Lett. **100**, 136406 (2008).

[36] A. I. Liechtenstein, V. I. Anisimov, and J. Zaanen, Density-functional theory and strong interactions: Orbital ordering in Mott-Hubbard insulators, Phys. Rev. B **52**, R5467 (1995).

[37] X. He, N. Helbig, M. J. Verstraete, and E. Bousquet, Tb2J: A python package for computing magnetic interaction parameters, Comput. Phys. Commun. **264**, 107938 (2021).

[38] N. Marzari and D. Vanderbilt, Maximally localized generalized wannier functions for composite energy bands, Phys. Rev. B **56**, 12847 (1997).

[39] A. A. Mostofi, J. R. Yates, G. Pizzi, Y.-S. Lee, I. Souza, D. Vanderbilt, and N. Marzari, An updated version of Wannier90: A tool for obtaining maximally-localised Wannier functions, Comput. Phys. Commun. **185**, 2309 (2014).

[40] H. Xiang, C. Lee, H.-J. Koo, X. Gong, and M.-H. Whangbo, Magnetic properties and energy-mapping analysis, Dalton Trans. **42**, 823 (2013).

[41] R. F. L. Evans, W. J. Fan, P. Chureemart, T. A. Ostler, M. O. A. Ellis, and R. W. Chantrell, Atomistic spin model simulations of magnetic nanomaterials, J. Phys.: Condens. Matter **26**, 103202 (2014).

[42] R. D. King-Smith and D. Vanderbilt, Theory of polarization of crystalline solids, Phys. Rev. B **47**, 1651 (1993).

[43] R. Resta, Macroscopic polarization in crystalline dielectrics: the geometric phase approach, Rev. Mod. Phys. **66**, 899 (1994).

[44] P.-W. Ma and S. L. Dudarev, Constrained density functional for noncollinear magnetism, Phys. Rev. B **91**, 054420 (2015).

[45] E. F. Bertaut, *Magnetism* (Academic Press, New York, 1963), Vol. 3.

[46] H. J. Zhao, J. Íñiguez, X. M. Chen, and L. Bellaiche, Origin of the magnetization and compensation temperature in rare-earth orthoferrites and orthochromates, Phys. Rev. B **93**, 014417 (2016).

[47] E. Bousquet and A. Cano, Non-collinear magnetism in multiferroic perovskites, J. Phys.: Condens. Matter **28**, 123001 (2016).